# Designing Ionic Conductive Elastomers Using Hydrophobic Networks and Hydrophilic Salt Hydrates with Improved Stability in Air

Burebi Yiming, Zhaoxin Zhang, Nasir Ali, Yuchen Lu, Shaoxing Qu, Shuze Zhu, Costantino Creton, Zheng Jia

# Designing ionic conductive elastomers using hydrophobic networks and hydrophilic salt hydrates with improved stability in air

*Burebi Yiming, Zhaoxin Zhang, Nasir Ali, Yuchen Lu, Shaoxing Qu, Shuze Zhu*, Costantino Creton*, Zheng Jia**

B. R. B Yiming, Z. X. Zhang, Y. C. Lu, Prof. S. X. Qu, Prof. S. Z. Zhu, Prof. Z. Jia
State Key Laboratory of Fluid Power and Mechatronic Systems
Key Laboratory of Soft Machines and Smart Devices of Zhejiang Province
Center for X-Mechanics
Department of Engineering Mechanics
Zhejiang University
Hangzhou 310027, China
E-mail: zheng.jia@zju.edu.cn; shuzezhu@zju.edu.cn

N. Ali
State Key Laboratory of Silicon Materials
Department of Physics
Zhejiang University
Hangzhou 310027, China

B. R. B Yiming, Prof. C. Creton
Sciences et Ingénierie de la Matierè Molle
ESPCI Paris, Université PSL, CNRS, Sorbonne Université
75005 Paris, France
Email: costantino.creton@espci.psl.eu

**Abstract:** Existing soft ionic conductors fall into two distinct categories: liquid-rich ionic conductors containing large amounts of liquid electrolytes (~70–90 wt% water for hydrogels and ~20–80 wt% ionic liquids for ionogels), and liquid-free ionic conductors that do not contain liquid components (e.g., ionic conductive elastomers). However, they are often plagued by dehydration, leakage of toxic ionic liquids, and air aging. We introduce here a novel hydrophobic/hydrophilic integrated design of soft ionic conductors that exhibit a small amount of water (~1–5 wt%) and thus improved stability of mechanical and electrical properties. Using hydrophobic polymer networks and hydrophilic salt hydrates, we synthesized ionic conductive elastomers (s-ICEs for short) containing only a tiny amount of bound water. Thanks to the small embedded water content, the s-ICEs are advantageous over liquid-rich ionic conductors in terms of enhanced mechanical/electrical stabilities and safety; they also outperform previously reported liquid-free ionic conductors by avoiding air-aging issues. The s-ICEs introduced here also show excellent stretchability, good elasticity, high fracture resistance, desirable optical transparency and ionic conductivity, which are comparable to those of state-of-the-art liquid-rich and liquid-free ionic conductors. With all above advantages, the s-ICE represents an ideal material for practical applications of soft ionotronics in ambient conditions for long-term applications.

The ionically conductive and mechanically soft nature of living matter has inspired the field of soft ionotronics, in which devices conduct electricity by employing both mobile ions and electrons[1]. Demonstrated examples of soft ionotronic devices include ionic spider webs[2], ionic touch pads[3,4], ionotronic luminescence[5], ionotronic fibers[6], triboelectric nanogenerators[7,8], etc. Intrinsically stretchable ionic conductors that can tolerate large deformations are highly desirable for the development of high-performance soft ionotronics. Based on the liquid content, there are two types of ionic conductors, namely, liquid-rich ionic conductors and liquid-free ionic conductors.

Liquid-rich ionic conductors, such as hydrogels containing dissolved salts and ionogels swollen by ionic liquids (ILs), which often contain over 90 wt% liquid electrolytes, have demonstrated unique characteristics of high ionic conductivity, excellent stretchability, and optical transparency. Broad applications have been demonstrated with liquid-rich ionic conductors in the area of bioelectronics[9,10], biomedical engineering[11], soft anti-fogging devices[12], sensing[13], energy harvesting[14], and ionotronic luminescent devices[15]. Nevertheless, liquids in such materials tend to leak and evaporate, which hampers the stable operation of liquid-rich ionic conductors over extended periods of time. For example, most hydrogels eventually suffer from dehydration even under ambient conditions, thereby reducing their elasticity and ionic conductivity and considerably limiting the durability of hydrogels as ionic conductors[16-18]. Ionogels, another representative of liquid-rich ionic conductors, are advantageous over hydrogels in terms of non-volatility, broad working temperature, and wide electrochemical window[19-21].

Still, many ionogels are plagued by the leakage of toxic ILs[22,23], especially when subjected to mechanical loadings such as squeezing, which may potentially lead to the corrosion of metal electrodes and safety-related issues due to the toxicity of ILs. Besides, the abundance of liquid components in liquid-rich ionic conductors may compromise the mechanical properties. For instance, the adhesion of hydrogels to various materials – from metals to elastomers and gels – is intrinsically problematic since load-carrying polymer chains are diluted and water molecules hardly transfer forces[24]. Moreover, ionogels face a trade-off between ionic conductivity and mechanical performance (i.e., modulus and strength) since the addition of ILs enhances the conductivity but typically reduces the stiffness and strength[13,22,25].

In recent years, liquid-free ionic conductors composed entirely of crosslinked polymer networks and mobile ions have emerged. The rapid advancement of the field is illustrated by the advent of ionic conductive elastomers (ICEs)[26-28], in which both cations and anions are mobile, and ionoelastomers[29], in which either anions or cations are fixed to the elastomer network while the other species of ions remain mobile. Existing liquid-free ionic conductors, however, suffer from limitations inherent to the hygroscopic nature of either the electrolytes or the hydrophilicity of the polymers. Many ionoelastomers either exhibit limited stretchability[29] or are opaque[30], such that they cannot meet the requirements of soft ionotronics such as optoelectronic devices and optical fibers, which require stretchability and optical transparency[31-33].

In the last few years, our group reported novel stretchable ionic conductors, including liquid-rich and liquid-free ionic conductors. We investigated the effect of combining different

electrolytes (e.g., different salts, and ionic liquids) in the same copolymer network of P (MEA-*co*-IBA). This copolymer network is an ideal backbone for ionic conductors, since it has excellent mechanical properties at room temperature and provides some degree of tunability through the monomer composition. To put our previous work in prospective, Figure 1 shows a map of the ionic conductivity versus strength of the two different systems synthesized from the same copolymer networks but different electrolytes. The ICEs developed based on the copolymer networks containing different lithium salts (i.e., LiTFSI and $LiClO_4$)[27,34] show a moderate ionic conductivity but a high mechanical strength (i.e., ~7MPa). Note that the strength and ionic conductivity could be increased simultaneously due to the interaction between the polymer networks and ions of electrolyte salt[27]. Unfortunately, such an excellent combination of properties is only stable in dry conditions. In other words, the hydrophilic nature of $Li^+$ ions in the electrolyte salt makes liquid-free ICEs moisture sensitive[34], resulted in an evolving (decreased) stiffness and stress at break over time due to the plasticizing effect of water[34]. Yet, stability in ambient air is essential for applications in the presence of oxygen and water. As a potential solution to this stability problem we developed copolymer networks swollen with hydrophobic ionic liquids such as $[C_2mim][NTf_2]$ and [BMMIm][TFSI] resulting in ambiently stable ionogels[16] but exhibiting a maximum strength of only ~ 0.7 MPa. Therefore ionic conductors combining both a high stress at break and a long-term ambient stability remain desirable in practical applications.

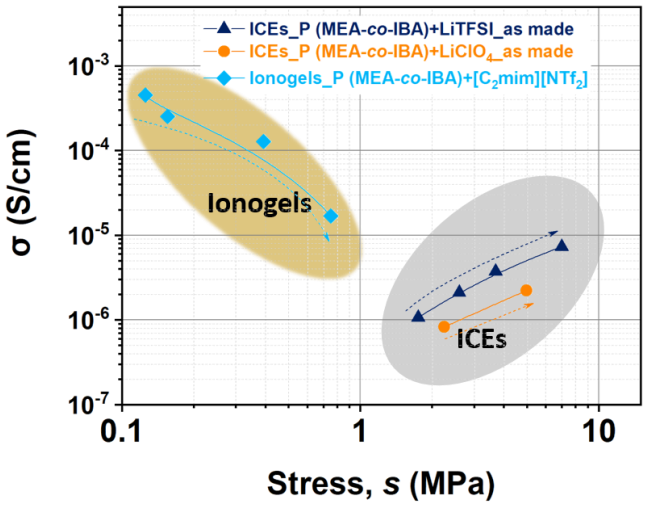


**Figure 1.** Ionic conductors (ICEs and ionogels ) made of P (MEA-*co*-IBA) copolymer networks. The direction of the arrows indicates the variation of the parameters (ionic conductivity and strength) with increased electrolyte content (i.e., either the lithium salts in the ICEs or the IL in the ionogels).

In this work, we report an ionic conductive elastomer (i.e., s-ICE) with hydrophobic/hydrophilic integrated design using P (MEA-*co*-IBA) hydrophobic polymer networks and hydrophilic salt hydrates. Unlike liquid-rich ionic conductors containing a large amount of liquid (~70–90 wt% water for hydrogels; ~20–80 wt% ILs for ionogels) and liquid-free ionic conductors having no liquid component, the s-ICEs reported here contain ~1–5 wt% of bound water molecules (Figure 2a), offering long-term stability in terms of mechanical and electrical properties under ambient conditions. Thanks to the ultralow water content, the s-ICEs represent a new soft ionic conductor that can be practically used in ambient conditions or open environments for long periods of time, since they overcome stability issues of existing ionic conductors – which are related to either high or zero liquid content – including but not limited to dehydration and the leakage of toxic ILs for liquid-rich ionic conductors in ambient and harsh

environments, as well as air aging issue and low conductivity for many typical liquid-free ICEs and ionoelastomers. The s-ICEs also demonstrate ultrahigh stretchability, high fracture toughness, good elastic recovery, and self-adhesiveness, which are comparable to those of state-of-the-art liquid-rich and liquid-free ionic conductors. With all above advantages, the s-ICEs containing ultralow water content are an ideal material for practical applications of soft ionotronics.

To prepare the s-ICEs, we use amorphous copolymer P(MEA-*co*-IBA) synthesized from acrylate monomers[35] – i.e., ethylene glycol methyl ether acrylate (MEA) and isobornyl acrylate (IBA) – as the hydrophobic polymer backbone, lithium perchlorate trihydrate ($LiClO_4 \cdot 3H_2O$) as the hydrophilic electrolyte salt, and benzophenone (BP) as the photoinitiator. The fabrication process of the s-ICEs includes a few steps: First, crystals of $LiClO_4 \cdot 3H_2O$ and BP are dissolved into MEA monomer, followed by the addition of IBA monomer to form a transparent precursor solution (Figure 2b). The molar ratio of IBA to MEA is fixed at 1:4, and the molar concentration of BP in the liquid binary mixtures of acrylate monomers (i.e., IBA plus MEA) is 0.0052 M. Subsequently, the precursor solution is polymerized into a transparent and stretchable s-ICE under an ultraviolet lamp (wavelength 365nm, light intensity ~4 $mWcm^{-2}$) for 7.5 h in a nitrogen environment. By tuning the molar concentration of $LiClO_4 \cdot 3H_2O$ in the binary mixture of acrylate monomers from 0.25 M to 1 M in a 0.25 M interval, a series of s-ICEs are synthesized. The obtained s-ICEs are named s-ICE-x, where x represents the molar concentration of the electrolyte salt $LiClO_4 \cdot 3H_2O$. For example, s-ICE-0.5 refers to an s-ICE containing 0.5 M $LiClO_4 \cdot 3H_2O$, and the prefix ***s*** represents stable. The choice of using $LiClO_4 \cdot 3H_2O$ as hydrophilic electrolyte salt

is the key point of this system. $LiClO_4 \cdot 3H_2O$ can easily dissolve in the hydrophobic liquid monomers used in this work and the bound water makes up ~34% of the mass of $LiClO_4 \cdot 3H_2O$, leading to an s-ICE system containing ~1–5 wt% of water. The glass transition temperature of the s-ICEs clearly decreases with increasing concentration of hydrated lithium salt as shown by the DSC scans (figure S1), suggesting that the salt is dissolved in the polymer networks. The composition of each sample is given in Table 1, including the weight and molar fractions of monomers, electrolyte salt, and water. In the following of this paper, we examine the physical properties of the s-ICEs and investigate how the ultralow water content contributes to enhancing the stability of mechanical and electrical performances of s-ICEs relative to their liquid-rich (i.e., hydrogels) and liquid-free counterparts (i.e., ICEs and ionoelastomers).

**Table 1. Composition of s-ICEs synthesized in this work.**

| Sample | Weight fraction of the components (wt%) | | | | Molar fraction of the components | | | |
|---|---|---|---|---|---|---|---|---|
| name | MEA | IBA | $LiClO_4$ | $H_2O$ | MEA | IBA | $LiClO_4$ | $H_2O$ |
| **s-ICE-0.25** | 68.18% | 27.27% | 3.01% | 1.53% | 68.20% | 17.04% | 3.69% | 11.06% |
| **s-ICE-0.5** | 65.22% | 26.09% | 5.77% | 2.93% | 59.43% | 14.85% | 6.43% | 19.28% |
| **s-ICE-0.75** | 62.50% | 25.00% | 8.29% | 4.21% | 52.66% | 13.16% | 8.54% | 25.63% |
| **s-ICE-1.0** | 60.00% | 24.00% | 10.61% | 5.39% | 47.28% | 11.82% | 10.23% | 30.68% |

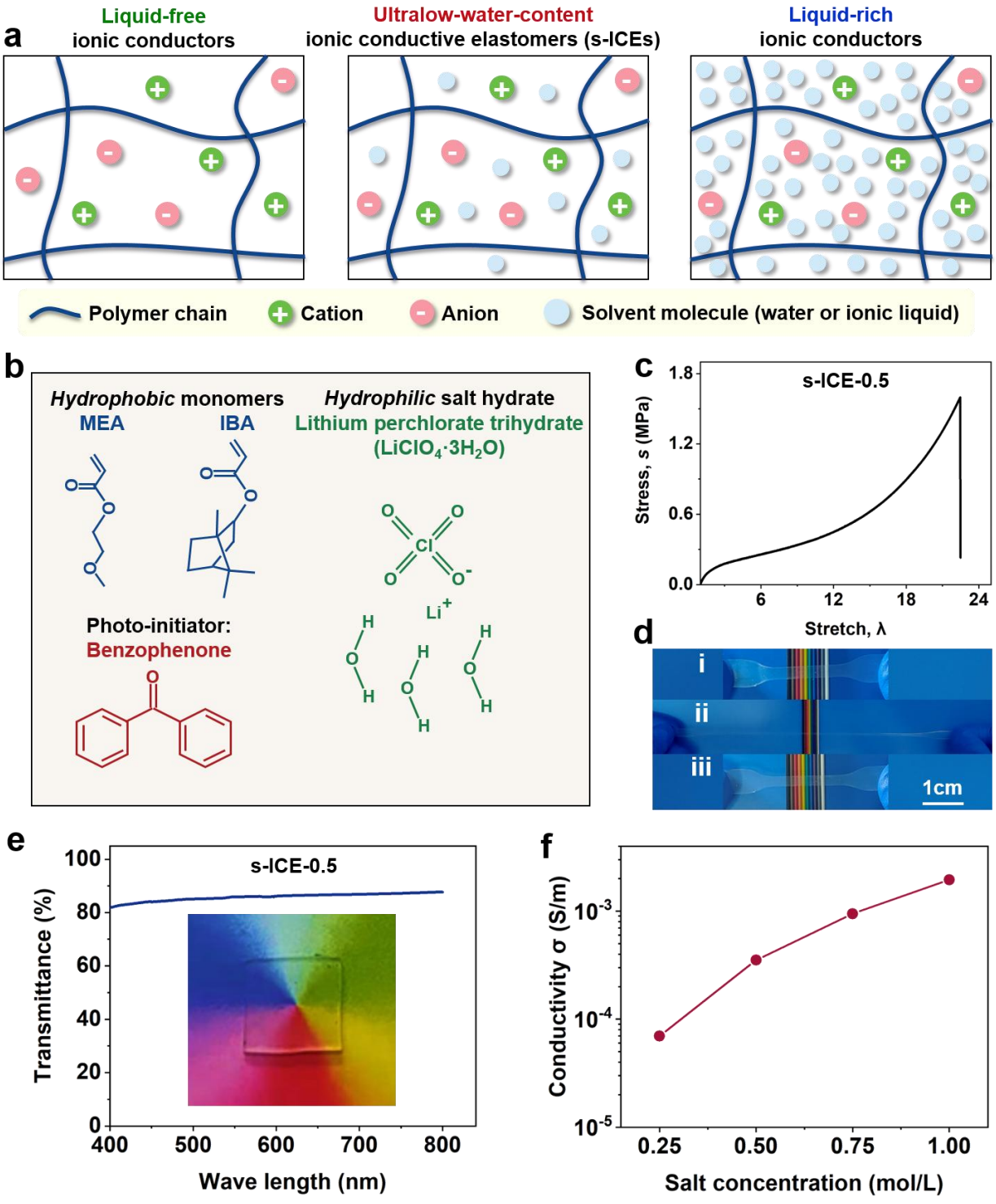


**Figure 2.** Synthesis and physical properties of the s-ICEs. (a) Schematic structures of the s-ICEs, liquid-free and liquid-rich ionic conductors. Liquid-free ionic conductors contain no liquid components while liquid-rich ionic conductors include a large amount of liquid electrolytes (~70–90 wt% water for hydrogels; ~20–80 wt%

ILs for ionogels). In contrast, the s-ICEs host about 1–5 wt% of water. (b) Chemical structures of MEA, IBA, the salt hydrate $LiClO_4 \cdot 3H_2O$, and photo-initiator BP. (c) A representative stress-strain curve of the s-ICE-0.5. The s-ICE-0.5 sample demonstrates a superb stretch capability with the stretch at break $\lambda_b = 22.48$. (d) Photographs of an s-ICE-0.5 before (ⅰ), during (ⅱ), and after stretching. After being stretched to roughly 10 times its original length, the sample almost recovers its original length immediately (Scale bar: 1 cm). (e) Transmittance in the visible range (wavelength 400–800 nm) of a 1 mm-thick s-ICE-0.5 sample. Inset: The 1 mm-thick s-ICE-0.5 sample placed on top of different colors. (f) Ionic conductivity of the s-ICEs with different $LiClO_4 \cdot 3H_2O$ concentrations.

The obtained s-ICEs exhibit high stretchability, excellent reversible elasticity, good transparency and ionic conductivity. Figure 2c shows that the s-ICE-0.5 exhibits an ultra-high stretchability with a stretch at break in uniaxial extension of $\lambda_b = 22.48$, being one of the most stretchable ionic conductors reported to date among both liquid-rich and liquid-free ionic conductive materials. The s-ICEs possess much enhanced stretch capability, strength and stiffness, relative to the pure copolymer P (MEA-*co*-IBA) that contains no lithium salt (Figure S2) due to the formation of physical bonds such as hydrogen bonds and lithium bonds between the ions of salt hydrates and polymer networks according to our previuos findings[27,34]. Moreover, the s-ICEs possess excellent elastic reversibility. For example, the s-ICE-0.5 can immediately recover its original length after being stretched to 10 times its original length and released (Figure 2d), demonstrating highly elastic behavior of the material. The s-ICEs are also optically transparent: a 1 mm-thick s-ICE-0.5 sample has an average transmittance of 85% over the entire visible range, as

shown in Figure 2e; the inset shows that the whole spectrum of visible colors can be seen through the s-ICE-0.5 sample. In addition, the s-ICEs present a desirable ionic conductivity at room temperature for soft ionotronic devices. As the concentration of $LiClO_4{\cdot}3H_2O$ increases from 0.25 M to 1 M, the ionic conductivity at room temperature of the s-ICEs can reach $1.95 \times 10^{-3}$ S m$^{-1}$ (Figure 2f), orders of magnitude higher than that of many existing liquid-free ICEs and ionoelastomers[26,29], because the existence of water molecules – though in very limited amount (i.e., 3 water molecules per lithium ion) – can effectively facilitate the motion of lithium ions[34].

To gain comprehensive insights into the mechanical behavior of the material, we perform uniaxial tensile tests on four series of s-ICEs with various $LiClO_4{\cdot}3H_2O$ concentrations (namely, 0.25 M, 0.5 M, 0.75 M, and 1 M). Intriguingly, all samples containing different salt concentrations exhibit a nearly identical stress-strain behavior (Figure S3) – independent of the concentration of $LiClO_4{\cdot}3H_2O$ – and all possess an extremely high stretchability, with stretch at break $\lambda_b > 21$ for all the cases tested (Figure 3a), higher than that of most previously reported ionic conductors[14,16,17,26,28,29,36]. Tensile strengths and Young's moduli of all series of s-ICEs extracted from the uniaxial tensile tests are on the same level (Figure 3b), regardless of the electrolyte salt concentration. Fracture behaviors of s-ICEs are also investigated systematically by quantitative measurements of both fracture toughness $\Gamma$ on notched samples ($\sim$4000 J/m$^2$) and work of fracture $W$ on unnotched samples ($\sim$12 MJ/m$^3$), respectively – for all four series of s-ICEs investigated (Figure 3c).

In our experiments, we surprisingly observe small or no differences in mechanical

performance and fracture toughness between the s-ICEs containing different content of salt hydrates. The reason behind this result may be due to two factors. First, interactions between polymer chains and ions of lithium hydrates, stiffen and strengthen the material[27,34] and (i.e., figure S2) while small amounts of bound water play the role of a plasticizer. When the concentrations of salt hydrates increase, both effects (i.e., the interaction between the polymer chains and ions of the hydrated salt and plasticizing effect of the bound water) vary simultaneously with opposite influences, resulting in no significant differences in bulk mechanical and fracture behavior of the material. Secondly, the differences in volume fraction of polymer, which affects the mechanical properties of the materials (table S1) are small. Small differences in the volume fractions of the s-ICEs leads to ignorable differences in the mechanical performances.

To investigate the level of reversible elasticity of s-ICEs, we carry out cyclic-loading tests of s-ICEs. In the first set of experiments, samples are stretched to a maximum stretch ratio of $\lambda_{max} = 11$ before unloading. All the samples exhibit nearly identical hysteresis loops and levels of energy dissipation, independent of the salt concentration (Figure 3d and 3e; Figure S4). The corresponding recovery ratio (defined as $1 - \varepsilon_{res}/\varepsilon_{max}$, where $\varepsilon_{res}$ is the residual strain and $\varepsilon_{max} = \lambda_{max} - 1$ is the maximum strain.) of all the s-ICEs exceeds 90% under a 100 mm/min displacement speed (the corresponding stretch rate = $0.14\ s^{-1}$), indicative of the highly reversible elastic behavior of the material at large deformations, regardless of the salt concentration (Figure 3e). In the second experiment, we cyclically stretch the s-ICE-0.5 samples to increasing maximum stretches – from $\lambda_{max} = 2$ to $\lambda_{max} = 13$. The s-ICEs demonstrate an

ultimate recovery ratio of ~90%, with a corresponding residual stretch of only $\lambda_{res} = 2.24$ after being released from $\lambda_{max} = 13$ (Figure 3f and Figure S5). The dissipated energy $U_d$ during each cycle increases almost linearly with $\lambda_{max}$ (Figure 3g). These results indicate a highly elastic behavior of s-ICEs with rapid elastic recovery and low hysteresis at high stretch ratio, a trait highly desirable for functional materials to find uses in soft ionotronics.

Soft ionotronic devices are highly integrated systems and are typically comprised of various materials with distinct functionalities. In such systems, robust interfacial adhesion between different components is a fundamental requirement, which dictates the overall structural integrity and reliability of such devices. Achieving strong interfacial adhesion of hydrogels (a typical liquid-rich ionic conductor) to other functional materials, however, has been challenging due to the abundance of water molecules[37], which changes neighbor readily and transmit forces negligibly. The adhesion energy of natural hydrogel-elastomers interface without special interfacial treatment is typically below 1 J/m$^2$ [38]; existing bonding methods that enable strong adhesion between hydrogels and elastomers are often restricted to specific chemistries[39-41]. Unlike conventional hydrogels, the s-ICEs reported here demonstrate instant tough bonding to a wide variety of materials – from hard to soft – with high interfacial toughness: the 90° peeling tests show that the adhesion energy between the s-ICEs and copolymers of P (MEA-*co*-IBA), glass, copper, and VHB are 752.6, 685.7, 502.5, and 93.3 J/m$^2$, respectively (Figure 3h and 3i). Owing to the self-adhesive nature of the s-ICEs, strong interfaces – including gel-copolymer, gel-glass, gel-copper, and gel-VHB – can be formed immediately by simply attaching s-ICEs to

surfaces of different materials. The interface can sustain large stretches $> 10$ without interfacial debonding, demonstrating a desirable level of adhesion of the s-ICEs to various surfaces (Figure S6).

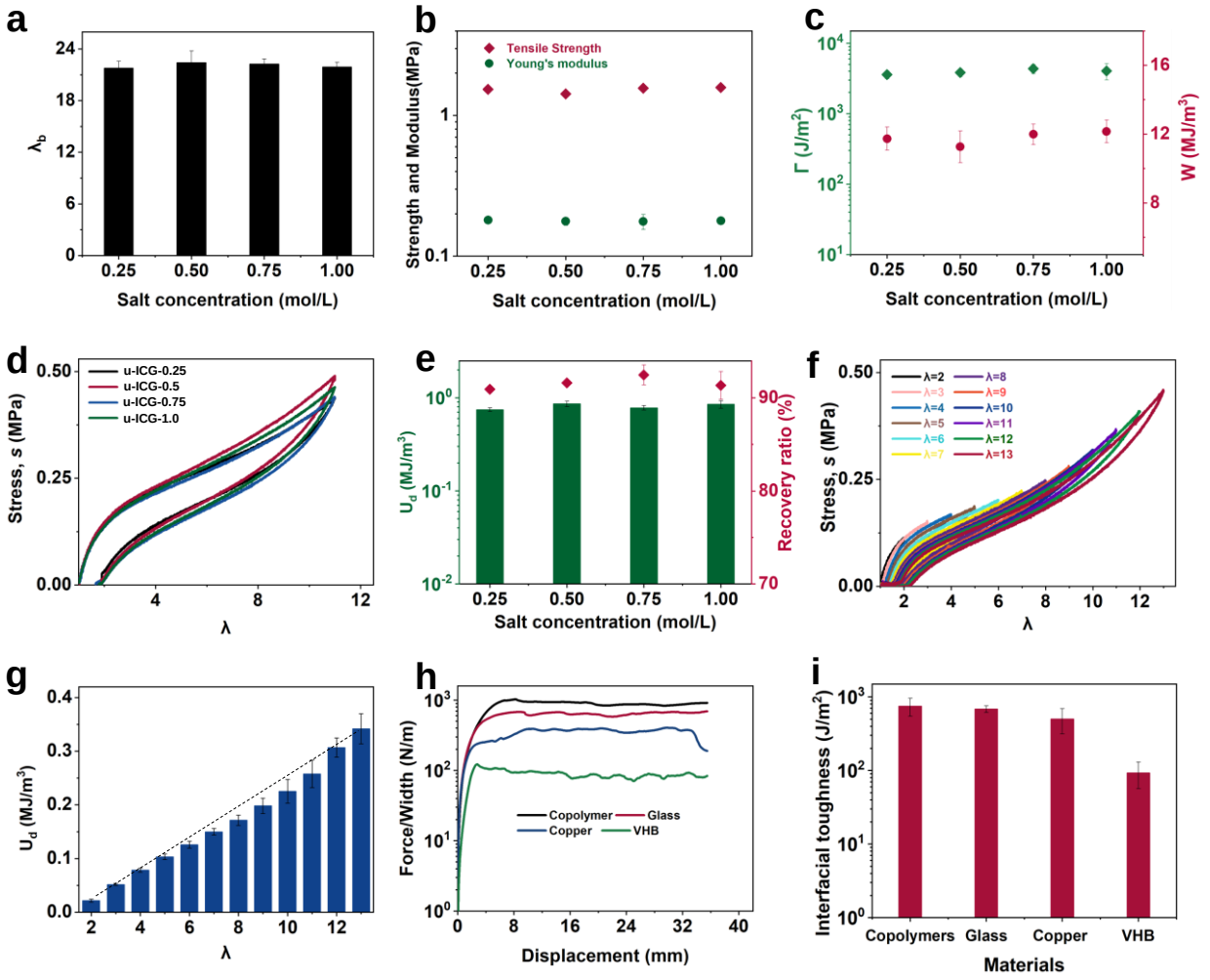


**Figure 3.** Mechanical properties of the s-ICEs. (a-b) Stretch at break $\lambda_b$, strength, and Young's modulus of the s-ICEs with different $LiClO_4 \cdot 3H_2O$ concentrations – from C=0.25 M to C=1 M. (c) Fracture toughness $\Gamma$ and work of fracture W of the s-ICEs containing different salt hydrate concentrations. (d) Representative loading-unloading curves with the maximum stretch $\lambda_{max} = 11$ for s-ICEs with different salt hydrate concentrations. A stretch rate of $0.14\ s^{-1}$ is employed. (e) The corresponding dissipation energy $U_d$ and the

recovery ratio for each s-ICE. The recovery ratio is defined as $1-\varepsilon_{res}/\varepsilon_{max}$, where $\varepsilon_{res}$ is the residual strain and $\varepsilon_{max}=\lambda_{max}-1$ is the maximum strain. (f) Successive loading-unloading curves of the s-ICE-0.5 cyclically stretched to different maximum stretches, which increase from $\lambda_{max}=2$ to $\lambda_{max}=13$. (g) The corresponding dissipation energy of the s-ICE-0.5 sample in each loading-unloading cycle. (h) Force-displacement curves of the s-ICE-0.5 samples obtained from the 90° peeling test, the plateau value of which gives the adhesion energy (i.e., interfacial toughness). (i) The corresponding adhesion energy of the s-ICE-0.5 to various materials, including the copolymer of P (MEA-*co*-IBA), glass, copper, and VHB.

It has been widely recognized that liquid-rich ionic conductors such as hydrogels and ionogels suffer from key limitations inherent to liquid electrolytes, which may leak under mechanical loadings[42], evaporate in a dry environment[18], or easily take in water molecules from surroundings [22], thereby changing the mechanical and electrical properties of the material. Liquid-free ionic conductors, including ICEs and ionoelastomers, contain no liquid component, avoiding the hassles of leaking liquid materials; however, many of them are prone to water absorption and hydroxylation and are subject to humidity-induced aging under ambient conditions[27,29]. To demonstrate the ambient stability of the s-ICEs, we expose s-ICE-0.5 samples to the ambient atmosphere (~30-50% relative humidity, RH) for 72 h and measure the stress-strain curves at 24 h intervals. The s-ICEs retain their mechanical properties during the entire testing period, which is indicative of the excellent structural stability of s-ICEs under ambient conditions (Figure 4a-c and Figure S7a). For comparison, we synthesize two types of liquid-free ICEs – P(MEA-*co*-IBA) networks containing lithium salt LiTFSI and $LiClO_4$,

respectively – and measure their stress-strain curves after storing them in ambient air for 24 h. The liquid-free ICEs exhibit degraded mechanical performance after 24 h of storage due to moisture absorption (Figure S8). More evidence of the air-aging behavior of liquid-free ICEs containing LiTFSI or $LiClO_4$ salt has been provided in the literature[34], revealing that water molecule-assisted lithium bond breakage is the underlying mechanism for the degradation of the mechanical properties of liquid-free ICEs under ambient conditions[34]. To further showcase the s-ICEs' tolerance to extremely dry conditions, we store s-ICE-0.5 samples in a humidity-free nitrogen environment (water content <<0.01 PPm, oxygen content <<0.01 PPm). It is observed that, after 72 h of storage, the s-ICE samples do maintain their mechanical properties (Figure 4a-c, Figure S7b), showing that the mechanical performance of the s-ICEs is insensitive to extremely dry conditions, in conspicuous contrast to liquid-rich ionic conductors, especially hydrogels[18].

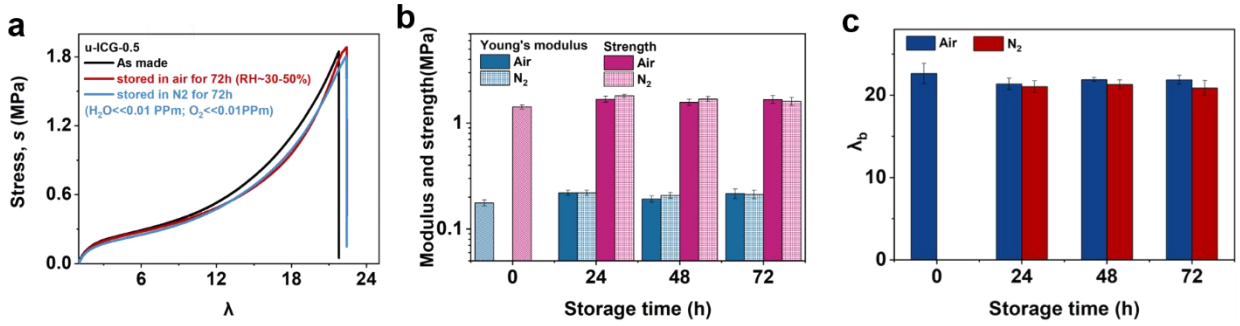


**Figure 4.** Stability of mechanical performance of s-ICEs under various conditions. (a) Representative stress-strain curves of as-made s-ICE-0.5 samples and samples after stored under ambient conditions and nitrogen atmosphere, respectively, for 72 h. The s-ICE demonstrates excellent stability in terms of mechanical performance under ambient and extremely dry conditions. (b-c) The evolution of Young's modulus, tensile

strength, and stretch at break $\lambda_b$ (stretchability) of s-ICE-0.5 samples during the 72 h of storage under ambient and extremely dry conditions. The values are measured at 24 h intervals

Changes in mechanical properties of liquid-rich gels and liquid-free ICEs are often related to leakage of liquids (i.e., water loss in hydrogels) or moisture absorption (i.e., water uptake of liquid-free ionic conductors). By contrast, the mechanical properties of the s-ICEs presented in this work appear relatively stable under dry and ambient conditions with varying humidity levels. To further confirm this result, we quantify the water content absorbed by the s-ICEs from environments with different humidity levels. Figure S9a displays the weight change of s-ICEs under ambient conditions, with the RH level changing from 30% to 70%. After 96 h storage, the s-ICEs gain negligible weight by water absorption – less than 0.1 wt% for all s-ICE samples, hardly affecting the mechanical properties of s-ICEs as demonstrated in Figure 4a-c. To gain comprehensive insights into the electrical performance of the s-ICEs, we examine the ionic conductivity of the s-ICEs under various RH levels. The s-ICEs demonstrate a relatively stable ionic conductivity for 30% < RH < 50% and exhibit a slightly higher ionic conductivity when the RH reaches ~70% (Figure S9b). This is in sharp contrast to nearly all liquid-rich hydrogels and some liquid-rich ionogels, which tend to lose ionic conductivity due to dehydration or the leakage of ILs[16,22,42]

Molecular dynamics simulations are conducted to explain the water retaining capability of s-ICEs under extremely dry conditions at the atomistic scale. For simplicity, we only consider modeling the MEA chains to represent the copolymer network because MEA is the majority

component. Figure 5a-b describes the simulation model. Twenty water molecules and one $LiClO_4$ molecule are embedded in the central region of a sphere-shaped MEA matrix, resembling a core-shell structure (illustrated in Figure 5a) where the core part is the $H_2O$-$LiClO_4$ cluster and the shell part is the MEA matrix (Figure 5b). In the simulation, the entire core-shell structure is subjected to a vacuum environment – much harsher than that in the glove box (namely, a dry nitrogen environment). All simulations are carried out at room temperature. The simulation results show that even under such harsh conditions, the $LiClO_4$ can effectively retain several water molecules. Figure 5c shows the time evolution of the spatial distance histogram accounting for the number of water molecules at certain distances away from the lithium ion, and the insets show the configurations of water molecules around the lithium ion at the corresponding moment. At the beginning of the simulation (i.e., at 0 ns), water molecules are dispersed around the lithium ion by the construction of the model. As the simulation time increases, the water molecules begin to diffuse outwards, which can be read from the evolving histogram (Figure 5c). If a water molecule has diffused to the surface of MEA shell, it is immediately removed in order to simulate the evaporation process. From the histograms, we can see that the longer the simulation time, the lesser the total number of water molecules. However, there are still 4~5 water molecules in close vicinity to the lithium ion (i.e., at the distance of 0.25 nm) after about 185 ns (see blue line in Figure 5d), in sharp contrast with the diminishing number of water molecules at other distances. This is a key signature of the water retaining capability of the s-ICE obtained from the simulation. To further clarify such an effect, we construct a control model in which the initial number of water

molecules is changed to 4, and find that these water molecules are not diffusing outwards and are bound closely to the lithium ion throughout the simulation (see green line in Figure 5d). By inspecting the simulation trajectories, it is found that the water retaining capability is due to lithium bonds formed between the oxygen atoms in the water molecules and the lithium ions. Lithium bonds are strong physical interactions able to attract water molecules, which is the reason why s-ICEs can retain water in extremely dry environments.

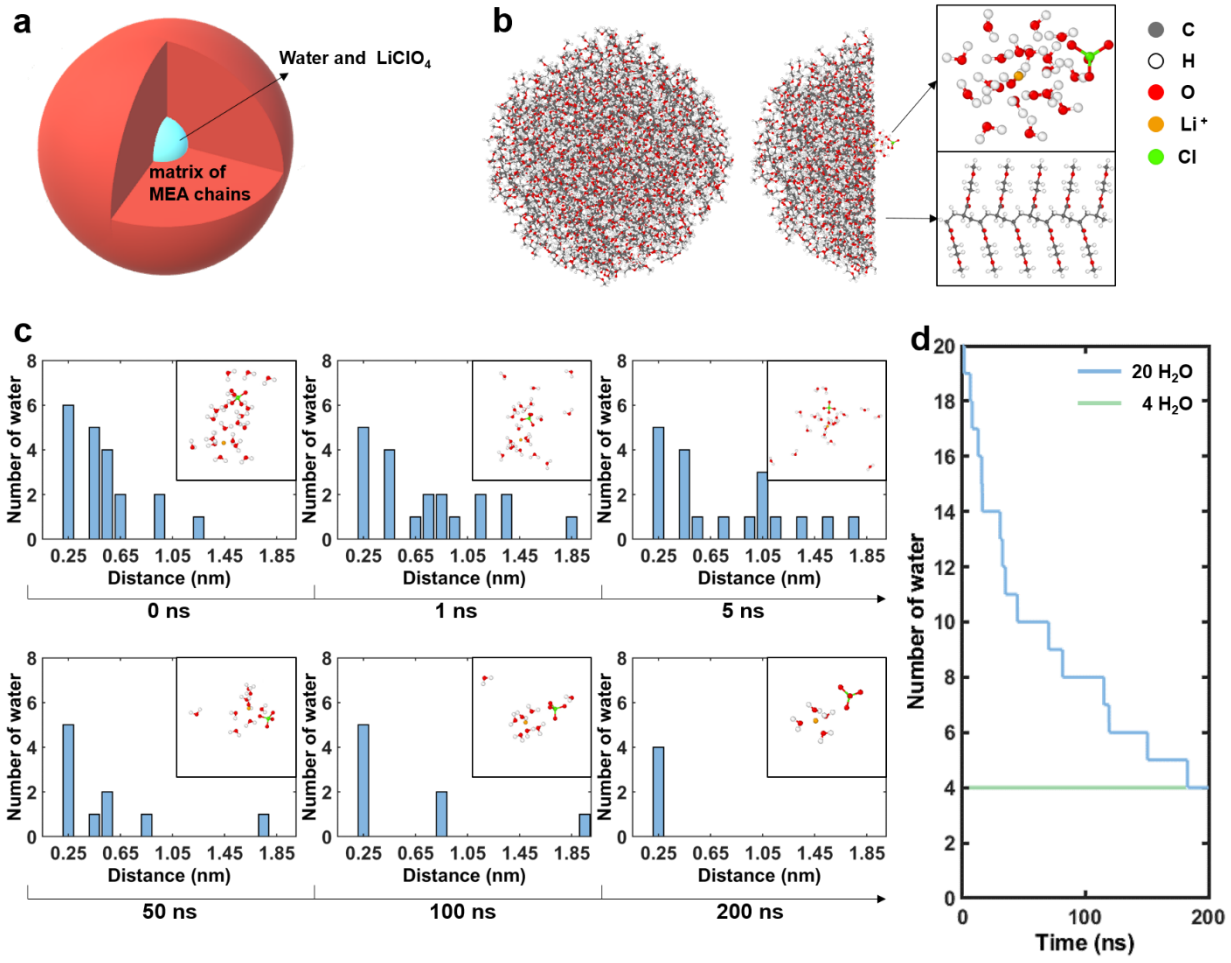


**Figure 5.** (a) 3D illustration of the simulation model. Water molecules and a $LiClO_4$ molecule are embedded in the central region of a sphere-shaped MEA matrix, resembling a core-shell structure. (b) Left shows the full view

of the atomistic simulation model. Right shows the view when half of the MEA matrix is removed to expose the core. (c) Time evolution of the spatial distance histogram accounting for the number of water molecules at certain distances away from the lithium ion. Insets are the corresponding configurations of water molecules around the lithium ion. (d) Time evolution of the total number of water in the model. The blue line represents the model with initially 20 water molecules. The green line represents the model with initially 4 water molecules. Both models show that the lithium ion can eventually retain 4 water molecules, demonstrating the water retaining capability of the s-ICEs under extremely dry conditions.

We also evaluate the electrical properties of a s-ICE-0.5 sample subjected to uniaxial tension. When the s-ICEs are stretched, the resistance increases nearly quadratically with increasing strain (Figure 6a). The result is well in line with the ideal elastomer model where the volume and resistivity of the material are taken to be fixed: When the s-ICE is stretched by a factor of $\lambda$, the cross-sectional area of the gel is reduced by a factor of $1/\lambda$, the resistance is thus $R/R_0 = \lambda^2$ [27], as shown in Figure 6a. The force-responsiveness of the s-ICEs makes it an ideal material for the design of a resistive sensor. Thus, we construct a simple resistive-type sensor by directly connecting metal conductive wires to the two ends of the s-ICE-0.5 strip. Cyclically stretching the sensor to different stretches of $\lambda = 1.5,\ 2,\ 2.5,\ 3,\ 3.5$ produces repeatable and strain-dependent resistance changes (Figure 6b). The sensing capability of the s-ICE-based sensor is further demonstrated by directly adhering the gel film to human fingers, and bending the finger to 90° produces a reliable resistance change signal (Figure 6c). In addition, the change in resistance of the s-ICE-based sensor exhibits excellent stability and repeatability

during cyclic stretching for 100 consecutive cycles to $\lambda_{max} = 3$ (Figure 6d), indicating its prominent durability.

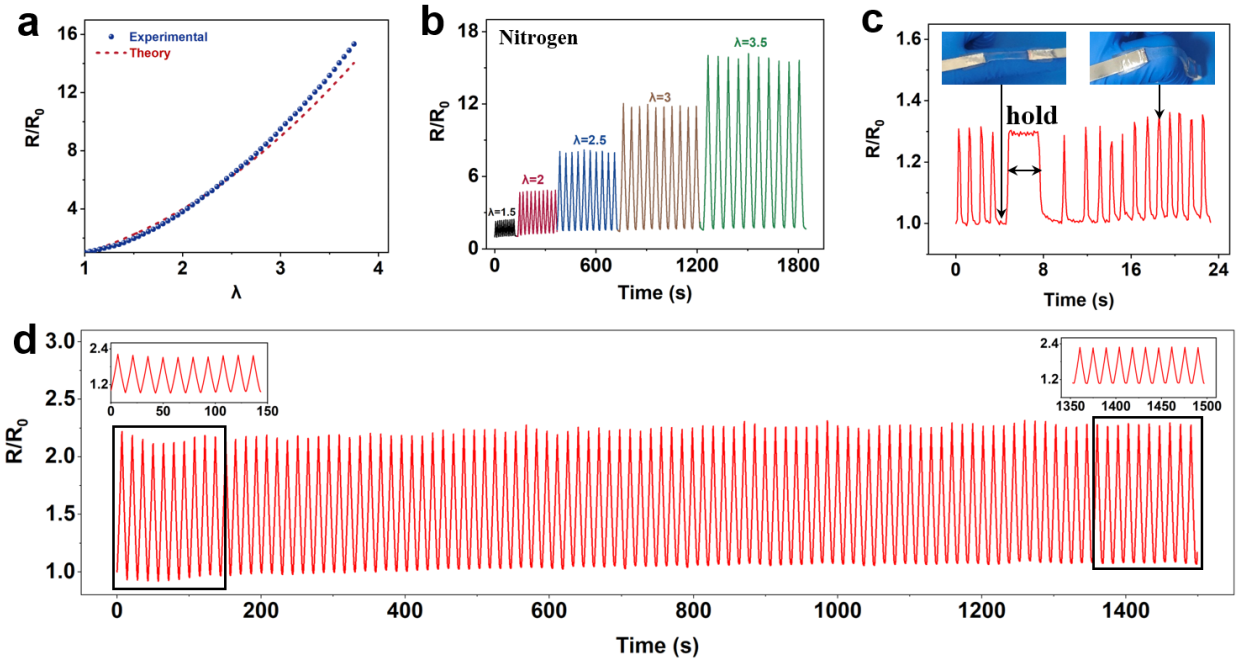


**Figure 6.** Electrical performance and applications of the s-ICEs. (a) Resistance changes versus stretches. The blue dots denote experimental data, in good agreement with the theoretical prediction represented by the dashed line. (b) Real-time response curves measured at fixed stretches of $\lambda_{max} = 1.5,\ 2,\ 2.5,\ 3, 3.5$ for ten cycles each. (c) The s-ICE-based strain sensor can accurately detect bending motion of human fingers. (d) Resistance variations of a s-ICE-based strain sensor subject to cyclic stretching ($\lambda_{max} = 3$) for 100 consecutive cycles.

Figure 7 shows the difference between different ionic conductors based on the same polymer networks of P (MEA-*co*-IBA), covering the ICEs containing different lithium salts (i.,e dry LiTFSI and $LiClO_4$, respectively)[27,34], ionogels based on the ionic liquid $[C_2mim][NTf_2]$[16], and the s-ICEs using hydrated salt introduced in this work. The design principles of these materials include:1) In all cases the monomer composition is kept the same and the absence of

crosslinker means that the materials are highly stretchable; 2) The two quantities that change depending on the additive (salt, hydrated slat, IL, water) are the stress at break and conductivity. The differences between the materials based on the different additives are: 1) The ICEs based on the dry lithium salts including LiTFSI and $LiClO_4$ exhibit the best mechanical strength but a lower ionic conductivity; 2) the ionogels possess the highest ionic conductivity and lowest mechanical strength among all; 3) the ionic conductivity and mechanical strength of the s-ICEs developed here by using hydrated lithium salts are a compromise between ICEs and ionogels (figure 7a). However, in addition the stability in the ambient conditions is important when it comes to the applications of the materials in the presence of water and oxygen under varying humidity levels. As figure 7b shows, The s-ICEs synthesized here using the salt hydrates exhibit a higher ionic conductivity ICE based on dry lithium salts and are stable over varying humidity levels for a long period of time under ambient air, while having a markedly higher strength than that of the corresponding ionogels.

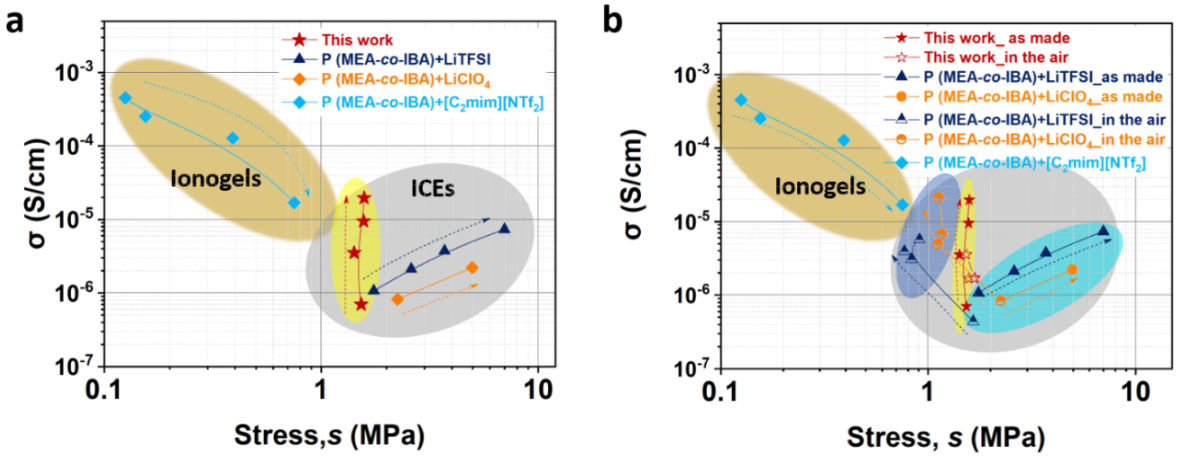


Figure 7. Ionic conductors (ICEs, ionogels, and s-ICEs ) made of P (MEA-*co*-IBA) polymer networks. a) Ionic

conductivity versus strength of the as made ICEs, ionogels, and s-ICEs, respectively. b) Ionic conductivity versus strength of the materials with the effect of ageing. We use the results of ICE_0.5 for both ICEs made of salt hydrates and dry salt (LiTFSI and $LiClO_4$) to show the effect of ambient water vapor on the evolution of the properties. The direction of the arrows indicates the variation of the parameters (ionic conductivity and strength) with increasing electrolyte content (i.e., lithium/hydrated lithium salts in the ICEs, ionic liquid in the ionogels ) in the as made state; For the aged samples, the directions of the arrows shows the change of the properties over time.

In conclusion, by using hydrophobic elastomer networks and salt hydrates, we report a new hydrophobic/hydrophilic integrated design of novel ionic conductors – the s-ICEs, which contain only a tiny amount of water (about 1–5 wt%), inherently different than existing ionic conductors that are either liquid-rich or liquid-free. Molecular dynamics simulations strongly suggest that the water present in s-ICEs in humid environments does not completely evaporate in dry environments. As evident by both experiments and molecular dynamics simulations, this small intrinsic water content of the s-ICEs imparts enhanced safety and environmental stability of both electrical and mechanical properties relative to liquid-rich ionic conductors (e.g., ionogels and hydrogels) and liquid-free ionic conductors under ambient conditions. The material also demonstrates excellent stretchability, good reversible elasticity, high fracture resistance, spontaneous adhesion to various surfaces, and desirable optical transparency. We finally demonstrate the use of s-ICEs as resistive-type stretch sensors. We hope that our work may inspire a series of new soft ionotronic devices with stable performance based the s-ICEs.

## Supporting Information

Supporting Information is available from the Wiley Online Library or from the author.


## Acknowledgments

We gratefully acknowledge the financial support from the National Key Technologies Research and Development Program (Grant No. 2022YFC3203900), Natural Science Foundation of Zhejiang Province (Grant No. LR22A020005), the National Natural Science Foundation of China (Grant No 12072314), and the 111 Project (Grant No. B21034). B.R.B. Yiming also thanks the financial support from the Chinese Scholarship Council (CSC).


## Conflict of Interest

The authors declare no conflict of interest.


## Keywords

Ionic conductive elastomers; ionic conductors; stability; hydrophilic; hydrophobic

## References


1 Canhui Yang, Zhigang Suo. Hydrogel ionotronics. *Nature Reviews Materials* **3**, 125-142, doi:10.1038/s41578-018-0018-7 (2018).

2 Younghoon Lee, Won Jun Song, Yeonsu Jung, Hyunjae Yoo, Man-Yong Kim, Ho-Young Kim, Jeong-Yun Sun. Ionic spiderwebs. *Science Robotics* **5**, eaaz5405, doi:DOI: 10.1126/scirobotics.aaz5405 (2020).

3 Chong-Chan Kim, Hyun-Hee Lee, Kyu Hwan Oh, Jeong-Yun Sun. Highly stretchable, transparent ionic touch panel. *Science* **353**, 682-686 (2016).

4 Mirza Saquib Sarwar, Yuta Dobashi, Claire Preston, Justin K. M. Wyss, Shahriar Mirabbasi, John David Wyndham Madden. Bend, stretch, and touch: Locating a finger on an actively deformed transparent sensor array. *Science Advances* **3**, e1602200 doi:doi:10.1126/sciadv.1602200 (2017).

5 Can Hui Yang, Baohong Chen, Jinxiong Zhou, Yong Mei Chen, Zhigang Suo. Electroluminescence of Giant Stretchability. *Advanced Materials* **28**, 4480-4484, doi:10.1002/adma.201504031 (2016).

6 Mingyue Yao, Baohu Wu, Xunda Feng, Shengtong Sun, and Peiyi Wu. A Highly Robust Ionotronic Fiber with Unprecedented Mechanomodulation of Ionic Conduction. *Advanced Materials* **33**, e2103755, doi:10.1002/adma.202103755 (2021).

7 Panpan Zhang, Yanghui Chen, Zi Hao Guo, Wenbin Guo, Xiong Pu, Zhong Lin Wang. Stretchable, Transparent, and Thermally Stable Triboelectric Nanogenerators Based on Solvent- Free Ion- Conducting Elastomer Electrodes. *Advanced Functional Materials* **30**, doi:10.1002/adfm.201909252 (2020).

8 Xiong Pu, Mengmeng Liu, Xiangyu Chen, Jiangman Sun, Chunhua Du, Yang Zhang, Junyi Zhai, Weiguo Hu, Zhong Lin Wang. Ultrastretchable, transparent triboelectric nanogenerator as electronic skin for biomechanical energy harvesting and tactile sensing. *Science Advances* **3**, e1700015, doi:doi:10.1126/sciadv.1700015 (2017).

9 Jue Deng, Hyunwoo Yuk, Jingjing Wu, Claudia E. Varela, Xiaoyu Chen, Ellen T. Roche, Chuan Fei Guo , Xuanhe Zhao. Electrical bioadhesive interface for bioelectronics. *Nature Materials* **20**, 229-236, doi:10.1038/s41563-020-00814-2 (2021).

10 Hyunwoo Yuk, Baoyang Lu, and Xuanhe Zhao. Hydrogel bioelectronics. *Chemical Society Reviewes* **48**, 1642-1667, doi:10.1039/c8cs00595h (2019).

11 Seongjun Park, Hyunwoo Yuk, Ruike Zhao, Yeong Shin Yim, Eyob W. Woldeghebriel, Jeewoo Kang, Andres Canales, Yoel Fink, Gloria B. Choi, Xuanhe Zhao, Polina Anikeeva. Adaptive and multifunctional hydrogel hybrid probes for long-term sensing and modulation of neural activity. *Nature Communications* **12**, 3435, doi:10.1038/s41467-021-23802-9 (2021).

12 Shaoting Lin, Yueying Yang, Jiahua Ni, Yoichiro Tsurimaki, Xinyue Liu, Baoyang Lu, Yaodong Tu, Jiawei Zhou, Xuanhe Zhao, and Gang Chen. Stretchable Anti- Fogging Tapes for Diverse Transparent Materials. *Advanced Functional Materials* **31**, doi:10.1002/adfm.202103551 (2021).

13 Cao Ziquan, Liu Hongliang, Jiang Lei. Transparent, mechanically robust, and ultrastable ionogels enabled by hydrogen bonding between elastomers and ionic liquids. *Materials Horizons* **7**, 912-918, doi:10.1039/c9mh01699f (2020).

14 Yongyuan Ren, Jiangna Guo, Ziyang Liu, Zhe Sun, Yiqing Wu, Lili Liu, Feng Yan. Ionic liquid–based

click-ionogels. *Science Advances* **5**, eaax0648 (2019).

15 C. Larson, B. Peele, S. Li, S. Robinson, M. Totaro, L. Beccai, B. Mazzolai, R. Shepherd. Highly stretchable electroluminescent skin for optical signaling and tactile sensing. *Science* **351**, 1071-1073, doi:DOI: 10.1126/science.aac5082 (2016).

16 Burebi Yiming, Xiao Guo, Nasir Ali, Nan Zhang, Xinning Zhang, Zilong Han, Yuchen Lu, Ziliang Wu, Xiulin Fan, Zheng Jia, and Shaoxing Qu. Ambiently and Mechanically Stable Ionogels for Soft Ionotronics. *Advanced Functional Materials* **31**, doi:10.1002/adfm.202102773 (2021).

17 Lei Shi, Kun Jia, Yiyang Gao, Hua Yang, Yaming Ma, Shiyao Lu, Guoxin Gao, Huaitian Bu, Tongqing Lu, and Shujiang Ding. Highly Stretchable and Transparent Ionic Conductor with Novel Hydrophobicity and Extreme-Temperature Tolerance. *Research* **2020**, 2505619, doi:10.34133/2020/2505619 (2020).

18 Yuanyuan Bai, Baohong Chen, Feng Xiang, Jinxiong Zhou, Hong Wang, and Zhigang Suo. Transparent hydrogel with enhanced water retention capacity by introducing highly hydratable salt. *Applied Physics Letters* **105**, doi:org/10.1063/1.4898189 (2014).

19 Jean Le Bideau, Lydie Viau and Andre Vioux. Ionogels, ionic liquid based hybrid materials. *Chemical Society Reviewes* **40**, 907-925, doi:10.1039/c0cs00059k (2011).

20 Haifei Wang, Ziya Wang, Jian Yang, Chen Xu, Qi Zhang, and Zhengchun Peng. Ionic Gels and Their Applications in Stretchable Electronics. *Macromolecular Rapid Communications*, e1800246, doi:10.1002/marc.201800246 (2018).

21 Daniela Maria Correia, Liliana Correia Fernandes, Pedro Manuel Martins, Clara García-Astrain, Carlos Miguel Costa, Javier Reguera, and Senentxu Lanceros-Méndez. Ionic Liquid–Polymer Composites: A New Platform for Multifunctional Applications. *Advanced Functional Materials* **30**, doi:10.1002/adfm.201909736 (2020).

22 Baohong Chen, Jing Jing Lu, Can Hui Yang, Jian Hai Yang, Jinxiong Zhou, Yong Mei Chen, and Zhigang Suo. Highly stretchable and transparent ionogels as nonvolatile conductors for dielectric elastomer transducers. *ACS Applied Materials and Interfaces* **6**, 7840-7845, doi:10.1021/am501130t (2014).

23 Błażej Kudłak, Katarzyna Owczarek, Jacek Namieśnik. Selected issues related to the toxicity of ionic liquids and deep eutectic solvents--a review. *Environ Sci Pollut Res Int* **22**, 11975-11992, doi:10.1007/s11356-015-4794-y (2015).

24 Hae-Ryung Lee, Chong-Chan Kim, and Jeong-Yun Sun. Stretchable Ionics - A Promising Candidate for Upcoming Wearable Devices. *Advanced Materials* **30**, e1704403, doi:10.1002/adma.201704403 (2018).

25 Yong Min Kim, & Hong Chul Moon. Ionoskins: Nonvolatile, Highly Transparent, Ultrastretchable Ionic Sensory Platforms for Wearable Electronics. *Advanced Functional Materials* **30**, doi:10.1002/adfm.201907290 (2019).

26 Lei Shi, Tianxiang Zhu, Guoxin Gao, Xinyu Zhang, Wei Wei, Wenfeng Liu & Shujiang Ding. Highly stretchable and transparent ionic conducting elastomers. *Nature Communications* **9**, 2630, doi:10.1038/s41467-018-05165-w (2018).

27 Burebi Yiming, Ying Han, Zilong Han, Xinning Zhang, Yang Li, Weizhen Lian, Mingqi Zhang, Jun Yin, Taolin Sun, Ziliang Wu, Tiefeng Li, Jianzhong Fu, Zheng Jia, and Shaoxing Qu. A Mechanically Robust and Versatile Liquid-Free Ionic Conductive Elastomer. *Advanced Materials* **33**, e2006111,

doi:10.1002/adma.202006111 (2021).

28 Panpan Zhang, Wenbin Guo, Zi Hao Guo, Yuan Ma, Lei Gao, Zifeng Cong, Xue Jiao Zhao, Lijie Qiao, Xiong Pu, and Zhong Lin Wang. Dynamically Crosslinked Dry Ion-Conducting Elastomers for Soft Iontronics. *Advanced Materials* **33**, e2101396, doi:10.1002/adma.202101396 (2021).

29 Hyeong Jun Kim, Baohong Chen, Zhigang Suo, Ryan C. Hayward. Ionoelastomer junctions between polymer networks of fixed anions and cations. *Science* **367**, 773–776, doi:DOI: 10.1126/science.aay8467 (2020).

30 Xinxin Qu, Wenwen Niu, Rui Wang, Zequan Li, Yue Guo, Xiaokong Liu and Junqi Sun. Solid-state and liquid-free elastomeric ionic conductors with autonomous self-healing ability. *Materials Horizons* **7**, 2994-3004, doi:10.1039/d0mh01230k (2020).

31 Darren J. Lipomi, Michael Vosgueritchian, Benjamin C-K. Tee, Sondra L. Hellstrom,, Jennifer A. Lee, Courtney H. Fox and Zhenan Bao. Skin-like pressure and strain sensors based on transparent elastic films of carbon nanotubes. *Nature Nanotechnology* **6**, 788-792, doi:10.1038/nnano.2011.184 (2011).

32 Jingjing Guo, Xinyue Liu, Nan Jiang, Ali K. Yetisen, Hyunwoo Yuk, Changxi Yang, Ali Khademhosseini, Xuanhe Zhao, and Seok-Hyun Yun. Highly Stretchable, Strain Sensing Hydrogel Optical Fibers. *Advanced Materials* **28**, 10244-10249, doi:10.1002/adma.201603160 (2016).

33 Byeong Wan An, Sanghyun Heo, Sangyoon Ji, Franklin Bien & Jang-Ung Park. Transparent and flexible fingerprint sensor array with multiplexed detection of tactile pressure and skin temperature. *Nature Communications* **9**, 2458, doi:10.1038/s41467-018-04906-1 (2018).

34 Burebi Yiming, Zhaoxin Zhang, Yuchen Lu, Xingang Liu, Costantino Creton, Shuze Zhu, Zheng Jia, and Shaoxing Qu. Molecular Mechanism Underpinning Stable Mechanical Performance and Enhanced Conductivity of Air-Aged Ionic Conductive Elastomers. *Macromolecules* **55**, 4665-4674, doi:10.1021/acs.macromol.2c00161 (2022).

35 Liang Chen, Tao Lin Sun, Kunpeng Cui, Daniel R. King, Takayuki Kurokawa, Yoshiyuki Saruwatari and Jian Ping Gong. Facile synthesis of novel elastomers with tunable dynamics for toughness, self-healing and adhesion. *Journal of Materials Chemistry A* **7**, 17334-17344, doi:10.1039/c9ta04840e (2019).

36 Jeong-Yun Sun, Xuanhe Zhao, Widusha R. K. Illeperuma, Ovijit Chaudhuri, Kyu Hwan Oh, David J. Mooney, Joost J. Vlassak & Zhigang Suo. Highly stretchable and tough hydrogels. *Nature* **489**, 133-136, doi:10.1038/nature11409 (2012).

37 Yu Shrike Zhang, Ali Khademhosseini. Advances in engineering hydrogels. *Science* **356**, doi:10.1126/science.aaf3627 (2017).

38 Jingda Tang, Jianyu Li, Joost J. Vlassak, and Zhigang Suo. Adhesion between highly stretchable materials. *Soft Matter* **12**, 1093-1099, doi:10.1039/c5sm02305j (2016).

39 Daniela Wirthl, R. P., Michael Drack, Gerald Kettlguber, Richard Moser,, Robert Gerstmayr, F. H., Elke Bradt, Rainer Kaltseis, Christian M. Siket, & Stefan E. Schausberger, S. H., Siegfried Bauer, Martin Kaltenbrunner. Instant tough bonding of hydrogels for soft machines and electronics. *Science Advances* **3**, e1700053 (2017).

40 Yuk, H., Zhang, T., Parada, G. A., Liu, X. & Zhao, X. Skin-inspired hydrogel-elastomer hybrids with robust interfaces and functional microstructures. *Nature Communications* **7**, 12028, doi:10.1038/ncomms12028

(2016).

41 Qihan Liu, G. N., Canhui Yang, Shaoxing Qu and Zhigang Suo. Bonding dissimilar polymer networks in various manufacturing processes. *Nature communications* **9**, 846, doi:10.1038/s41467-018-03269-x (2018).

42 Zhouyue Lei, Peiyi Wu. A highly transparent and ultra-stretchable conductor with stable conductivity during large deformation. *Nature Communications* **10**, 3429, doi:10.1038/s41467-019-11364-w (2019).